

Search for gamma-ray bursts above 20 TeV with the HEGRA AIROBICC Cherenkov array

L. Padilla¹, B. Funk², H. Krawczynski^{3,4}, J.L. Contreras¹, A. Moralejo¹, F. Aharonian³, A.G. Akhperjanian⁵, J.A. Barrio^{1,6}, J.G. Beteta¹, J. Cortina¹, T. Deckers⁷, V. Fonseca¹, H.-J. Gebauer⁶, J.C. González^{1,6}, G. Heinzlmann⁴, D. Horns⁴, H. Kornmayer⁶, A. Lindner⁴, E. Lorenz⁶, N. Magnussen², H. Meyer², R. Mirzoyan^{5,6}, D. Petry^{2,6}, R. Plaga⁶, J. Prahl⁴, C. Prosch⁶, G. Rauterberg⁷, W. Rhode², A. Röhring⁴, V. Sahakian⁵, M. Samorski⁷, D. Schmele⁴, W. Stamm⁷, B. Wiebel-Sooth², M. Willmer⁷, and W. Wittek⁶

¹ Facultad de Ciencias Físicas, Universidad Complutense, E-28040 Madrid, Spain

² BUGH Wuppertal, Fachbereich Physik, Gaußstrasse 20, D-42119 Wuppertal, Germany

³ Max-Planck-Institut für Kernphysik, P.O. Box 103980, D-69029 Heidelberg, Germany

⁴ Universität Hamburg, II. Institut für Experimentalphysik, Luruper Chaussee 149, D-22761 Hamburg, Germany

⁵ Yerevan Physics Institute, Yerevan, Armenia

⁶ Max-Planck-Institut für Physik, Föhringer Ring 6, D-80805 München, Germany

⁷ Universität Kiel, Institut für Experimentelle und Angewandte Physik, D-24098 Kiel, Germany

Received 6 April 1998 / Accepted 13 May 1998

Abstract. A search for gamma-ray bursts (GRBs) above 20 TeV within the field of view (1 sr) of the HEGRA AIROBICC Cherenkov array (29°N, 18°W, 2200 m a.s.l.) has been performed using data taken between March 1992 and March 1993. The search is based on an all-sky survey using four time scales, 10 seconds, 1 minute, 4 minutes and 1 hour. No evidence for TeV-emission has been found for the data sample. Flux upper limits are given. A special analysis has been performed for GRBs detected by BATSE and WATCH. Two partially and two fully contained GRBs in our field of view (FOV) were studied. For GRB 920925c which was fully contained in our FOV, the most significant excess has a probability of $7.7 \cdot 10^{-8}$ (corresponding to 5.4σ) of being caused by a background fluctuation. Correcting this probability with the appropriate trial factor, yields a 99.7% confidence level (CL) for this excess to be related to the GRB (corresponding to 2.7σ). This result is discussed within the framework of the WATCH detection.

Key words: gamma rays: bursts – ISM: cosmic rays

1. Introduction

Emission of TeV/PeV gamma-rays associated with GRBs has been extensively searched. These studies are motivated by both the experimental results obtained with the satellite experiments as e.g. EGRET and by theoretical models (Meszaros et al. 1994) which predict or at least allow TeV emission to be produced in GRBs. So far none of these searches have revealed any convincing evidence for VHE emission (see for example Aglietta et al. 1993; Alexandreas et al. 1994; Borione et al. 1995; Connaughton et al. 1997; Dazeley et al. 1997), although

some tentative positive evidence has been found recently in this energy range (Plunkett et al. 1995; Krawczynski et al. 1995; Amenomori et al. 1996).

Up to now five BATSE GRBs have been detected by EGRET with photons of energies up to 18 GeV (Hurley et al. 1994). Those GRBs are among the most intense ones recorded by BATSE in the FOV of EGRET, so observations are compatible with the hypothesis that all GRBs emit GeV photons but only the strongest ones are above the EGRET sensitivity. A simple power law extrapolation of the Superbowl GRB spectrum (Sommer et al. 1994) predicts that ~ 20 photons above 20 TeV should be observed with the extensive air shower (EAS) array of wide angle integrating Cherenkov counters (AIROBICC) within 25 seconds while expecting only 0.1 background events. This would lead to a highly significant detection by several other experiments currently operating (Cherenkov telescopes, EAS arrays). The previous extrapolation neglects source-intrinsic cutoffs and the attenuation through interaction with the low energy cosmic photon background (Wdowczyk et al. 1972; Mannheim et al. 1996; Stecker & de Jager 1997), which is expected for cosmological sources with redshift greater than 0.1. Another interesting feature of strong GRBs is that their high energy emission can be delayed and have longer durations than keV–MeV emission (Hurley et al. 1994). These ideas motivate searches for counterparts at times and with durations independent of those given by the space detectors at lower energies, especially when considering that the latter could miss GRBs out of their FOV, or with a very hard spectrum, as has been already suggested (Piran & Narayan 1995; see also Kommers et al. 1997). Searches for GRBs with the HEGRA experiment using other data periods can be found in Krawczynski (1997), Funk (1997), Padilla et al. (1997), Krawczynski et al. (1998), Padilla (1998).

Send offprint requests to: padilla@gae.ucm.es

2. The AIROBICC array

The AIROBICC array is part of the cosmic ray (CR) HEGRA detector complex located at the Roque de los Muchachos on the Canary Island La Palma (28.75° N, 17.89° W, 2240 m a.s.l.). It is an array of 7x7 stations (currently enlarged to 8x8 plus a subarray of 4x4 to increase detector density in the center) with a regular grid spacing of 30 m, thus covering more than 32000 m². Each station consists of a 40 cm diameter reflecting cone which focuses the incoming light onto a fast 20 cm diameter photomultiplier tube (PMT). The set is placed inside a protective hut with a lid which can be opened through remote control. The PMT is covered with a blue filter ($\lambda = 300\text{-}480$ nm) to improve signal to noise ratio (S/N). The PMT output is amplified in the hut and sent through a 150 m long cable to a constant fraction discriminator (CFD) placed in the electronics container. The CFD is set to a level equivalent to 5σ of the night sky background fluctuations. Whenever six or more AIROBICC stations exceed the CFD threshold within 200 ns, a trigger is produced. Calibrations are performed every 20 minutes to measure the relative delay between stations, the response of the TDC and the ADC pedestals. The mean dead time after each recorded event is ~ 8 ms. Detailed descriptions of AIROBICC and the other components of the HEGRA complex can be found in Karle et al. 1995a, Fonseca et al. 1995a, Fonseca et al. 1995b.

The ADC signals (AIROBICC + scintillator array) are used to locate the EAS core position with a typical error ≤ 18 m. The Cherenkov light front is fitted by a cone to determine the arrival direction of the incident CR. The angular resolution (angular distance containing 63% of events for a point source) is 0.29° when 12 stations are fired (standard cut) and it continuously improves with increasing number of triggered huts. The absolute pointing accuracy has been estimated through comparison with the first HEGRA Cherenkov telescope to be better than 0.2° (Karle et al. 1995a). The FOV, which is limited by the acceptance of the Winston cone, is 1 sr and the trigger rate is ~ 20 Hz. The energy threshold (50% trigger probability) is estimated to be $\sim 16(25)$ TeV for γ s and $\sim 29(37)$ TeV for hadrons with zenith angle $\theta \leq 20^\circ$ ($20^\circ < \theta < 35^\circ$) using flux and Monte Carlo studies (Martínez et al. 1995). The price that has to be paid for the advantages of the Cherenkov technique (lower energy threshold, better angular resolution) is that observations are restricted to moonless clear nights ($\sim 10\%$ duty cycle).

3. Analysis

The data analyzed in this work were taken during the first year of operation of AIROBICC, between March 1992 and March 1993. The mean trigger rate in this period was ~ 16 Hz. The sample contains $\sim 4 \cdot 10^7$ events (~ 800 hours) and after a successful arrival direction reconstruction of those showers with ≥ 7 fired stations, about $\sim 2.5 \cdot 10^7$ events ($\sim 60\%$) survive. It has been shown that due to the low counting statistics encountered when dealing with transient phenomena, one has to keep as many events as possible; and so we do not apply the standard cut in the number of fired huts. The angular resolution is then $\sim 0.6^\circ$.

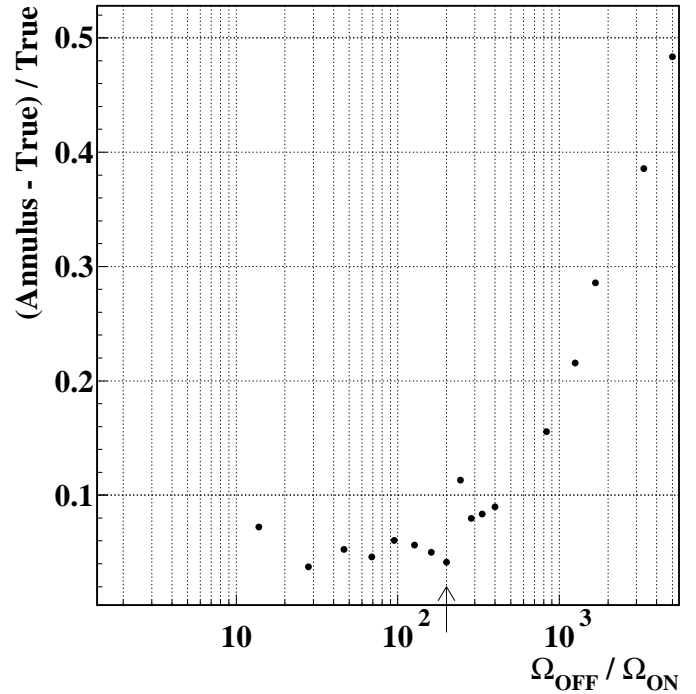


Fig. 1. Systematic error in the estimate of the background with the annulus method as a function of the ratio of the solid angles of the OFF and ON windows. The ON window is a fixed circle of 0.7° radius and the OFF window is an annulus of fixed 1.5° inner radius and variable outer radius. The time interval is 4 minutes which is expected to have the lowest statistical error. The points are the average over several hundred windows. The sample used for this calculation consists of MC events generated as described in the text. The systematic error has a constant value of less than 5% up to a certain size of the OFF window, from which it grows very fast. The arrow points to the value used in this work. This error has to be balanced against the statistical error which in the best case is 20%. Note that the sign of the systematic error is positive, i.e. it is conservative.

The analysis is based on a binned (in time and in space) all-sky search. We define an ON window or source window and an OFF window or background window where events are counted for a certain time interval. The search strategy considers each event as being in the middle (in time) of a burst, so for every single event in the data sample we take a pair of ON-OFF windows with a time interval centered at the time of the event. The ON window is a circle of 0.7° radius centered at the position of the event and the OFF window is an annulus of 1.5° and 10.0° radii concentric to the ON window. The solid angles covered by the ON and OFF windows are denoted by Ω_{ON} and Ω_{OFF} respectively, and their ratio $\Omega_{\text{ON}}/\Omega_{\text{OFF}}$ by α . There is always one event inside the ON window and in order to not overestimate the significance of a possible signal this event is not counted. The size of the ON window is chosen to maximize the S/N according to our resolution (see above) as described in Alexandreas et al. (1993a) and it is expected to contain 75% of the events for a point source. While the size of the OFF window is taken as large as possible to increase statistics, its limit is due to the systematic error introduced because of the non-linear

Table 1. 90% confidence level upper limits for the integral flux (in units of $10^{-8} \text{ cm}^{-2} \text{ s}^{-1}$) of any hypothetical GRB occurred in our data sample. They are tabulated depending on the time window and the declination band. Uncertainties are $\sim 40\%$.

Time scale	10 sec	1 min	4 min	1 hour
$F_{UL}(E > 16\text{TeV})$ ($9^\circ < \delta < 49^\circ$)	4.5	3.5	2.5	0.35
$F_{UL}(E > 25\text{TeV})$ ($-6^\circ < \delta < 9^\circ$, $49^\circ < \delta < 64^\circ$)	2.8	2.2	1.6	0.32

dependence of the counting rate on zenith angle (Alexandreas et al. 1993a). We performed a Monte Carlo (MC) calculation to find the largest radius that keeps the systematic error much lower than the statistical error due to the low counting rate. Results are shown in Fig. 1. The time intervals we chose are 10 seconds, 1 minute and 4 minutes which cover the usual long duration GRBs. Dead time and low counting rate do not allow searches for GRBs with much shorter duration.

The employed procedure has the advantage of being very sensitive but it is also quite time consuming. So in order to look for TeV-emission on longer time scales, a less sensitive search with a 1 hour time window and a classical non-overlapping rectangular grid of $0.5^\circ \times 0.5^\circ$ in celestial coordinates has been carried out. In this case the background is estimated by means of a MC method as described in Alexandreas et al. (1993a). For every real event we generate 100 MC events with random directions following the acceptance function of AIROBICC (obtained with the events of a whole run, therefore a different run implies a different acceptance function) but with the same times as that of the original event. The number of MC events that fall within the ON window determines the background.

To obtain the significance for a hypothetical signal we use the probability distribution given in Alexandreas et al. (1993a) which is appropriate for low statistics (Poissonian regime). It is the probability of observing at least N_{ON} events in the source window, given the observed number of background events N_{OFF} , as a result of a background fluctuation:

$$P(\geq N_{ON} | N_{OFF}) = 1 - \sum_{n_{ON}=0}^{N_{ON}-1} \frac{\alpha^{n_{ON}}}{(1+\alpha)^{n_{ON}+N_{OFF}+1}} \frac{(n_{ON} + N_{OFF})!}{n_{ON}! N_{OFF}!}$$

where N_{ON} and N_{OFF} are the number of events in the source and background windows respectively. In case of random distribution of the events (i.e., no GRBs), a cumulative histogram of the number of trials with a chance probability lower than P as a function of $-\log_{10}P$ should follow a straight line with slope -1, which cuts the Y-axis at the height of the total number of windows (trials). A strong GRB or several weaker GRBs should therefore appear as a deviation from the line. The significance of a deviation can be calculated knowing that theoretically every bin content follows a binomial distribution. Actually this approach is only an approximation because the probability distribution is discrete and there is an oversampling (i.e., search

Table 2. List of GRBs observed in coincidence with satellites. θ is the zenith angle of the GRB at the AIROBICC site.

GRB	Observer	θ at trigger	θ 2 ^h later	Coverage
920525b	BATSE	10.0°	31.4°	Full
920925c	WATCH	5.1°	25.1°	Full
921118	BATSE	27.6°	44.9°	Partial
930123	BATSE	29.6°	10.0°	Partial

windows overlap and thus trials are not independent) in the search with short time windows. Therefore we estimate the significance repeating the search over a MC sample which is 10 times larger than the real one in the case of short time windows and 20 times larger in the case of 1 hour search window.

4. Results

The results for the all-sky search are shown in Fig. 2. It presents the cumulative number of trials (search windows) against $-\log_{10}P$ for the all-sky search with the four time scales we have used. The results for the MC sample are also shown. Obviously, the experimental data set is consistent with MC expectations. The set of deviations has a chance probability greater than ~ 0.1 . This result allows us to place an upper limit for the flux of any hypothetical GRB which may have occurred in the FOV during our observations. Depending on the declination band the resulting upper limit corresponds to two energy thresholds for every time scale.

Assuming the same spectral index for the source and the CR flux and a steady emission during the time interval, we can estimate the integral flux upper limit with the formula (Karle et al. 1995b; Alexandreas et al. 1993b)

$$F_{UL}(E > E_{th_\gamma}) = \frac{N_{UL}\Omega_{ON}}{\alpha(N_{OFF} + 1)\beta} F_{CR}(E > E_{th_{had}})$$

where F_{UL} is the 90% CL upper limit for the integral flux, E_{th_γ} and $E_{th_{had}}$ are the energy thresholds for γ and hadrons respectively, N_{UL} is the 90% CL upper limit for the number of excess events in the source window as calculated by Aguilar-Benítez et al. (1992) and β is the fraction of source events expected to fall in the source window. F_{CR} is the known CR integral flux and is taken as $1.8 \cdot 10^{-5} E(\text{TeV})^{-1.76 \pm 0.09} \text{ cm}^{-2} \text{ s}^{-1} \text{ sr}^{-1}$ (Alexandreas et al. 1993b; Burnett et al. 1990). We applied this calculation to all ON-OFF windows and determined the highest values. The resulting flux upper limits are listed in Table 1. Their uncertainties are estimated to be $\sim 40\%$ through comparison with a different method of flux calculation.

Additional constraints on the data sample as e.g. imposed by the burst detections of BATSE, WATCH and other GRB detectors in space, can serve as a tool to reduce the full data set and thus the expected statistical fluctuations. Hence, the sensitivity is enhanced allowing detection of weaker GRBs. We therefore searched in the BATSE 3B catalog (Meegan et al. 1995) and in the WATCH catalog (Castro-Tirado 1994; Sazonov et al. 1997) for triggers which were within the FOV of AIROBICC at the time they occurred or up to 2 hours later (because of possible

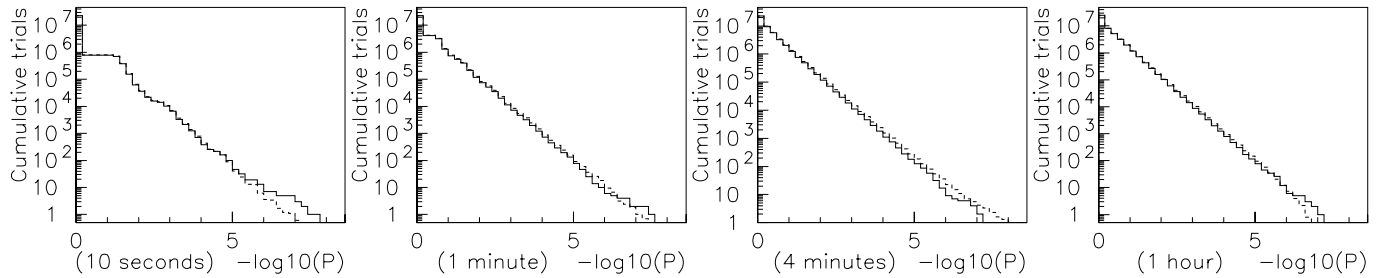


Fig. 2. Cumulative number of trials (windows) versus probability in the all-sky search. The time scale is indicated in brackets. The solid lines represent real data while the dashed lines represent the results (normalized to the real data) over a MC sample 10 (20 in the 1 hour scale) times larger than the real one. Deviations are not significant ($p \leq 0.1$).

Table 3. 90% confidence level upper limits for the integral flux (in units of $10^{-10} \text{ cm}^{-2} \text{ s}^{-1}$) of GRB 920525b in different time scales and for two scenarios: coincident and delayed emission. Uncertainties are $\sim 40\%$.

Time scale	10 sec	1 min	4 min	1 hour
$F_{UL}(E > 16\text{TeV})$ (coincident, ± 3 min)	89	8.9	3.2	0.40
$F_{UL}(E > 16\text{TeV})$ (delayed, $< 2^h$ later)	130	14	3.2	—

delayed emission). They are shown in Table 2. The sample is then reduced to events within $\pm 10^\circ$ and ± 3 minutes around GRB locations. We also looked for a delayed component for two hours after the initial triggers. The size of the search region in celestial coordinates has been chosen, a priori, large enough to have the uncertainties of GRB locations into account. The length in time of the search interval (for coincident and delayed emission) has been taken according to the observations in the GeV energy range (Hurley et al. 1994).

The most significant excess in the full data set was found almost in coincidence with WATCH GRB 920925c, but from a direction 9° away from the most probable WATCH position. This observation is discussed in the next section. The results for the other three GRBs are shown in Fig. 3. It presents the cumulative number of trials against $-\log_{10}P$ for the four time scales used in the two search strategies (coincident and delayed emission). The results for the MC sample are shown as a dashed line. No significant deviation is seen. This, again, allows us to place an upper limit for the integral flux of these GRBs. However, we only do so for GRB 920525b because it is the only one completely covered by the data set among the three GRBs. The upper limits for the integral flux are calculated at 90% CL in the same way as shown before. The results for the coincident and delayed emission with the four time scales used here are shown in Table 3. Their uncertainties are estimated to be $\sim 40\%$.

5. Observational results for WATCH GRB 920925c

As it was mentioned in the previous section, the search for emission from GRB 920925c had a surprising result. An excess was found searching for emission in coincidence with the WATCH

trigger on all short time scales. No excess has been found either in the search for delayed emission or in the 1 hour time window. The results for the four time scales, in the two search modes (coincident and delayed emission), are shown in Fig. 4. Again the cumulative number of trials is plotted as a function of $-\log_{10}P$ and the dashed line shows the results for the MC sample. In this case significant deviations from the expectations are observed, especially in the 4 minute time scale (coincident emission), which shows a deviation with a chance probability $< 10^{-4}$.

The search interval with the smallest chance probability (4 minutes time scale, coincident emission) is centered at $\alpha = 324.6^\circ \pm 0.3^\circ$, $\delta = 16.8^\circ \pm 0.3^\circ$ (J2000) and UT = 22:45:21. Therefore it precedes the WATCH trigger by less than one minute and is about 9° away from the WATCH location. For this search interval we observe 11 events in 4 minutes while 0.93 events are expected. The chance probability for the background to yield such an excess, computed according to the formula shown above, is $7.7 \cdot 10^{-8}$ and the Li and Ma significance (Li & Ma 1983) is 5.4σ (in both cases we take into account only 10 events inside the search interval, see above). This is the most significant excess seen in the whole data sample (compare Fig. 4 with Fig. 2). Correcting this probability with a trial factor (using the MC) due to the search for the four GRBs in Table 2 on several time scales and in a large solid angle region, yields a final probability of $3.3 \cdot 10^{-3}$ (2.7σ), i.e. the CL for this excess to be related to WATCH burst is 99.7% (neglecting the possibility of a second independent burst). The data registered with the HEGRA scintillator array does not show any excess, which may be due to its higher energy threshold and worse angular resolution. The time distribution of the events registered by AIROBICC in the position of the excess for the night of the GRB is plotted in Fig. 5. The distribution of the 11 events yielding the smallest chance probability is shown in detail in the inner part of the figure. Note that 7 out of the 11 burst events come within 22 seconds, 3 of which arrive within 0.25 seconds.

Assuming that this excess is due to high energy emission we can calculate the integral flux in the same way as the upper limits, but replacing N_{UL} with $N_{ON} - \alpha(N_{OFF} + 1)$. In this case the tentative mean integral flux above 16 TeV during the 4 minutes window is $(9 \pm 4) \cdot 10^{-10} \text{ cm}^{-2} \text{ s}^{-1}$.

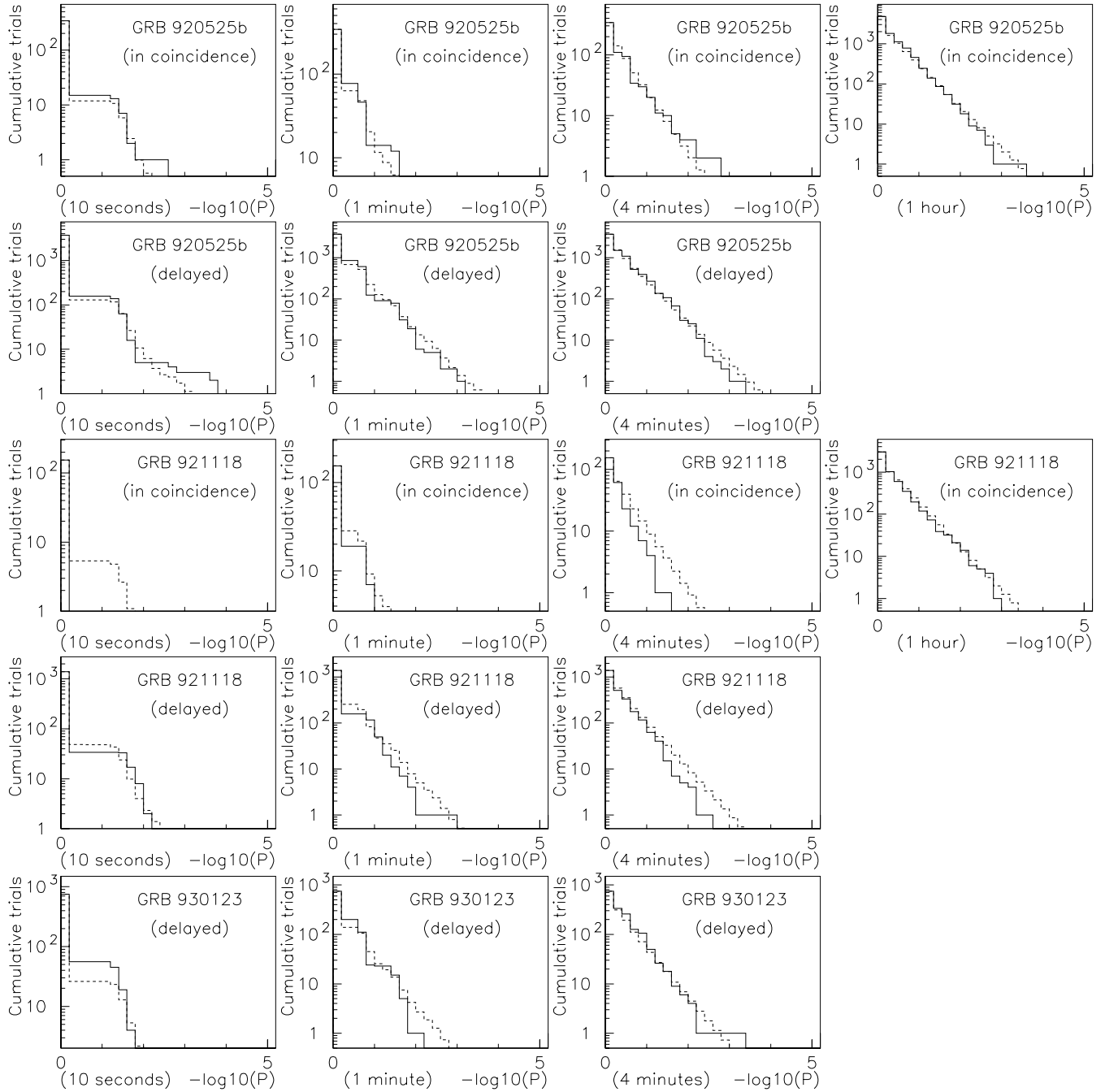


Fig. 3. Cumulative trials vs. probability in the search for the GRBs 920525b, 921118 and 930123. We show the results of the search for coincident and delayed emission. For GRB 930123 only the result for delayed emission is shown because AIROBICC started more than one hour after the burst trigger. The dashed line shows the MC results. No significant deviation appears.

The burst as seen by the space detectors had a duration of ~ 5 minutes exhibiting two main peaks. It was observed by WATCH and ULYSSES, thus reducing the possible locations to an IPN (InterPlanetary Network) annulus (Hurley 1996). This annulus is obtained using the relative time of detection of both spacecrafts. The IPN ring passes through the WATCH 3σ error circle and is 3° away from the excess observed with the AIROBICC array, see Fig. 6.

Spectral data from WATCH in the interval 6-100 keV can be fitted by a power law spectrum. The fit yields a spectral index of 2.5 ± 0.2 which, if naively extrapolated, does not predict any TeV flux detectable by AIROBICC. However, the TeV spectrum may differ significantly from what one expects from the 100 keV extrapolation. Furthermore, the hypothetical emission at TeV energies precedes the WATCH observations and may therefore be due to another production mechanism.

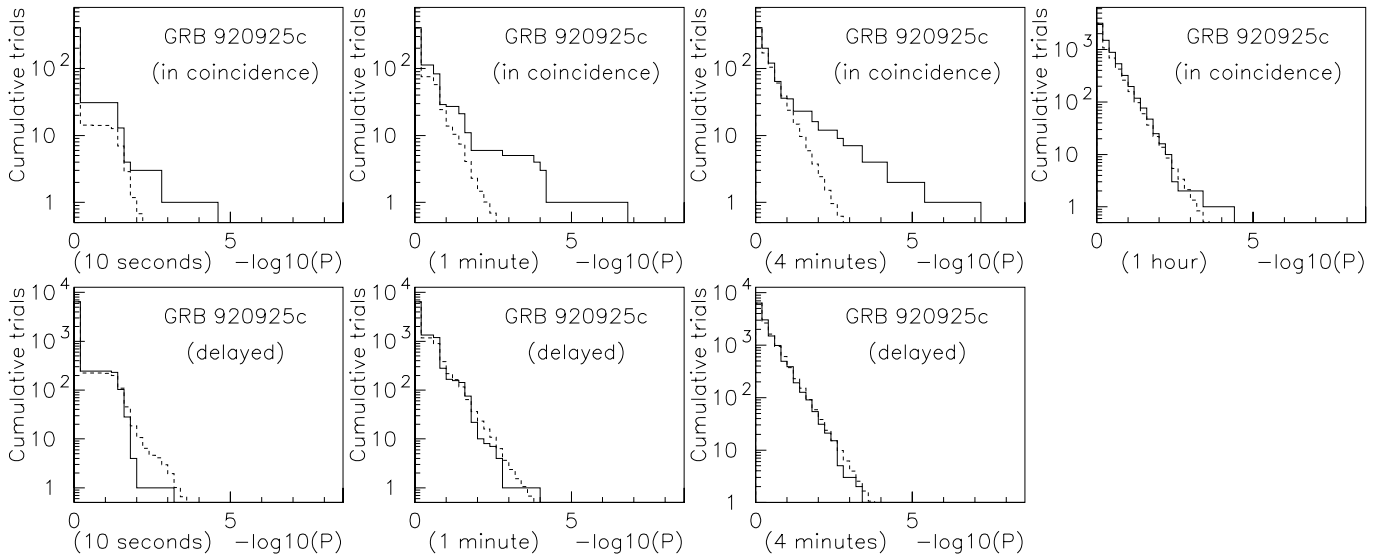


Fig. 4. Cumulative number of trials (windows) versus probability in the search for GRB 920925c. We show the results of the search for coincident and delayed emission. The dashed line shows the MC results. A significant deviation appears in some of the plots.

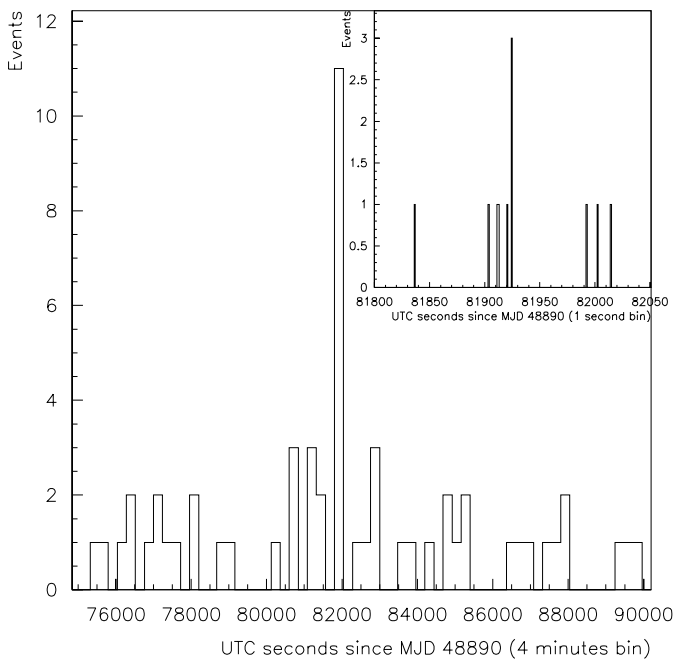


Fig. 5. Counting rate of events in the position of the excess detected by AIROBICC in coincidence with GRB 920925c along the four hours of moonless night. A clear peak is seen at the time of the excess, the inner figure shows in detail the time distribution of the burst events.

6. Discussion

In order to add new clues that may clarify whether the excess recorded with AIROBICC is related to GRB 920925c or not, the BATSE team (Kippen 1996) investigated the reason why BATSE was not triggered by this GRB. There are two reasons why BATSE may have missed the burst: either it was not strong enough to overwrite the previous trigger (happened about one hour before) or the Earth (or the Moon) occulted the source. The

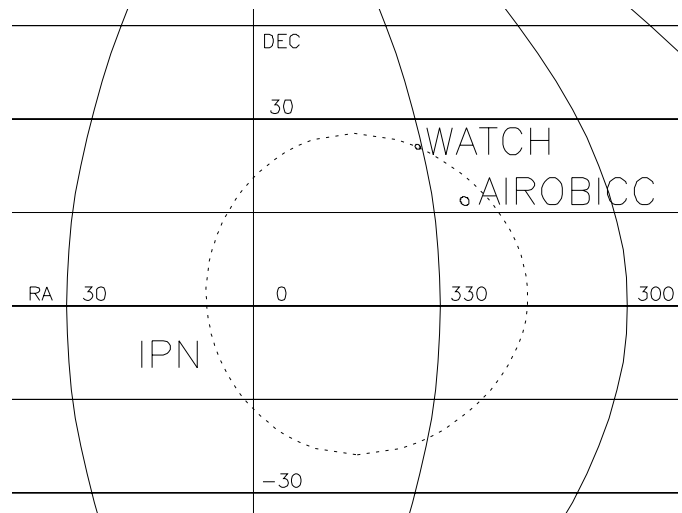


Fig. 6. Map with the situation of the WATCH GRB 920925c and the IPN ring as calculated from the WATCH and ULYSSES observations. The location of the excess detected by AIROBICC nearly coincident in time with WATCH is also shown.

BATSE team kindly provided us with a map of the sky, as seen by BATSE (Kippen 1996), at the time that GRB 920925c occurred. It shows that the AIROBICC location was completely occulted by the Earth throughout the whole burst. Therefore the AIROBICC observation is compatible with BATSE not seeing the GRB. The WATCH position was on the Earth's limb at the beginning of the burst and was occulted about one minute later. The first peak of GRB 920925c (which is within the first minute after the initial trigger) had lower peak flux than the previous BATSE trigger and thus it would have not produced a trigger overwrite even neglecting the additional attenuation by the Earth's atmosphere. So the position given by WATCH is also consistent with the non-detection of the GRB with BATSE.

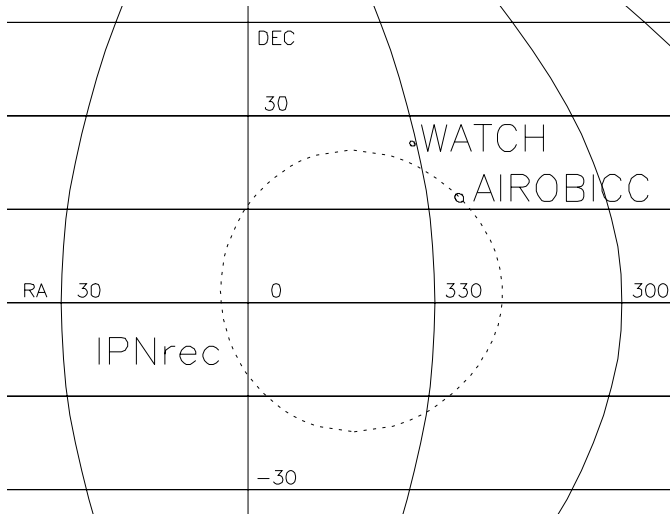


Fig. 7. Map with the situation of the WATCH GRB 920925c and the AIROBICC excess. The recalculated IPN ring using the ULYSSES and AIROBICC times of detection (see text) is also shown (IPNrec).

A cross-check of burst positions given by BATSE, WATCH and IPN since 1991 to 1994 reveals disagreements for some events at a level of 5σ or even more, so an error in the WATCH location cannot be discarded (if the error is due to timing it would also affect the IPN location estimate). Furthermore it is interesting to note that assuming that the peak registered with AIROBICC corresponds to the peak which triggered ULYSSES, we can recompute the IPN ring using the time of detection of AIROBICC (neglecting the WATCH-AIROBICC distance compared to the ULYSSES-Earth distance) yielding a new IPN ring which is compatible with AIROBICC but not with WATCH (see Fig. 7).

At this moment it is not possible to decide the nature of the excess recorded with AIROBICC. Note that this GRB had a large fluence at keV energies, but was not very intense. The GRB occurred under a small zenith angle (12°) and could thus be studied with a low energy threshold of the AIROBICC array. The events of the excess differ significantly from background events as shown in Fig. 8. The figure plots the mean of the ratio of scintillator fired huts to AIROBICC fired huts for groups of 11 events. The histogram fitted by a Gaussian function represents the groups of background events. The vertical dashed line, which is at 2.0σ as given by the Gaussian fit, represents the mean for the 11 events of the excess. It has been shown (Arqueros et al. 1996) that the ratio particles to light for EAS at observation level is sensitive to the chemical composition and the difference observed in Fig. 8 points to a gamma origin of the excess. This is confirmed by a MC study in which simulated EAS are analyzed in the same way as real data (Martínez et al. 1995; Cortina 1997). The results for real data and for MC are summarized in Table 4. If the excess has indeed gamma-ray nature its significance would be higher due to the much lower diffuse gamma-ray background compared to the charged particles background (Karle et al. 1995c). On the other hand the

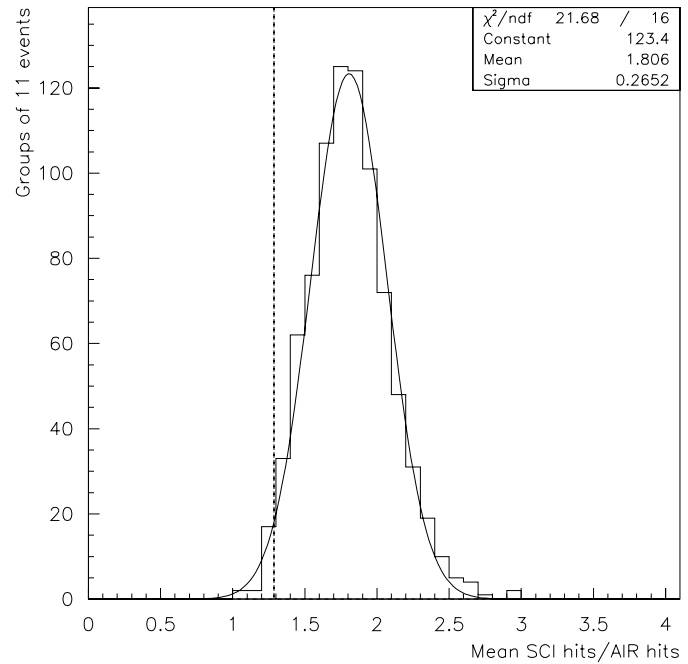


Fig. 8. Difference between the events of the excess and background in the ratio of fired huts in the scintillator and AIROBICC arrays for groups of 11 events. The mean for the 11 events of the excess (vertical dashed line) is below the mean for background groups (Gaussian fit) at a level of 2.0σ . The implications of this result are discussed in the text.

Table 4. Comparison between the ratio of scintillator fired huts to AIROBICC fired huts for groups of 11 events as predicted by the MC and as seen in the excess and in the background of the real data. The MC seems to confirm a gamma origin of the excess.

<SCI/AIR>	MC		Data	
	gammas	hadrons	excess	background
Mean	1.26	1.74	1.29	1.81
RMS	0.17	0.23	—	0.27

angular separation between AIROBICC and WATCH locations is significant.

Acknowledgements. The HEGRA Collaboration thanks the Instituto de Astrofísica de Canarias for the use of the HEGRA site at the Roque de los Muchachos and its facilities. We also thank the BATSE, ULYSSES and WATCH teams for the availability of their data. We are especially grateful to A. J. Castro-Tirado, J. Gorosabel, K. Hurley, M. Kippen and S. Y. Sazonov. This work was supported by the BMBF, the DFG, the CICYT and a grant from the MEC.

References

- Aglietta, M., et al., 1993, Proc. 23rd ICRC Calgary 1, 61.
- Aguilar-Benítez, M., et al. (PDG), 1992, Phys. Rev. D Rev. of Part. Prop. 45, 32.
- Alexandreas, D.E., et al., 1993a, NIM A328, 570.
- Alexandreas, D.E., et al., 1993b, ApJ 405, 353.
- Alexandreas, D.E., et al., 1994, ApJ 426, L1.
- Amenomori, M., et al., 1996, A&A 311, 919.

- Arqueros, F., et al., 1996, *Astropart. Phys.* 4, 309.
- Borione, A., et al., 1995, *Proc. 24th ICRC Rome* 2, 116.
- Burnett, T.H., et al., 1990, *ApJ* 349, L25.
- Castro-Tirado, A.J., 1994, Ph.D. Thesis, University of Copenhagen.
- Connaughton, V., et al., 1997, *ApJ* 479, 859.
- Cortina, J., 1997, Ph.D. Thesis, University Complutense of Madrid.
- Dazeley, S.A., et al., 1997, *Proc. 25th ICRC Durban* 3, 65.
- Fonseca, V., et al., 1995a, *Proc. 24th ICRC Rome* 1, 470.
- Fonseca, V., et al., 1995b, *Proc. 24th ICRC Rome* 1, 474.
- Funk, B., 1997, Ph.D. Thesis, University of Wuppertal.
- Hurley, K., et al., 1994, *Nat* 372, 652.
- Hurley, K., 1996, private communication.
- Karle, A., et al., 1995a, *Astropart. Phys.* 3, 321.
- Karle, A., et al., 1995b, *Astropart. Phys.* 4, 1.
- Karle, A., et al., 1995c, *Phys. Lett. B* 347, 161.
- Kippen, M., 1996, private communication.
- Kommers, J.M., et al., 1997, *ApJ* 491, 704.
- Krawczynski, H., et al., 1995, *Proc. 3rd Huntsville Symposium on GRB*.
- Krawczynski, H., 1997, Ph.D. Thesis, University of Hamburg.
- Krawczynski, H., et al., 1998, to be submitted to the *ApJ*.
- Li, T., Ma, Y., 1983, *ApJ* 272, 317.
- Mannheim, K., Hartmann, D., Funk, B., 1996, *ApJ* 467, 532.
- Martínez, S., et al., 1995, *NIM A* 357, 567.
- Meegan, C.A., et al., 1995, *Third BATSE Burst Catalog*, Compton Observatory Science Support Center, <http://coss.gsfc.nasa.gov/coss/BATSE.html>.
- Meszaros, P., Rees, M.J., Papathanassiou, H., 1994, *ApJ* 432, 181.
- Padilla, L., 1997, *Proc. 25th ICRC Durban* 3, 57.
- Padilla, L., 1998, Ph.D. Thesis in preparation, University Complutense of Madrid.
- Piran, T., Narayan, R., 1995, *Proc. 3rd Huntsville Symposium on GRB*.
- Plunkett, S.P., et al., 1995, *Ap&SS* 231, 271.
- Sazonov, S.Y., et al., 1997, to appear in *A&A*.
- Sommer, M., et al., 1994, *ApJ* 422, L63.
- Stecker, F.W., de Jager, O.C., 1997, *ApJ* 476, 712.
- Wdowczyk, J., Tkaczyk, W., Wolfendale, A.W., 1972, *J. Phys. A* 5, 1419.